Biosensors and Bioelectronics 133 (2019) 205–214

Contents lists available at ScienceDirect

Biosensors and Bioelectronics

journal homepage: www.elsevier.com/locate/bios

Ultra-selective fiber optic SPR platform for the sensing of dopamine in synthetic cerebrospinal fluid incorporating permselective nafion membrane and surface imprinted MWCNTs-PPy matrix

Anisha Pathak, Banshi D. Gupta*

Department of Physics, Indian Institute of Technology Delhi, New Delhi 110016, India

ARTICLE INFO

Keywords:
Optical fiber
Sensor
Dopamine
Surface plasmon
Molecular imprinting
Multiwalled carbon nanotube
Polypyrrole
Nafion

ABSTRACT

Surface plasmon resonance (SPR) based dopamine sensor is realized using the state-of-art technique of molecular imprinting over an optical fiber substrate. Polypyrrole (PPy) is depicted as an effective polymer for the imprinting of dopamine through a green synthesis approach. Sensitivity of the probe is enhanced by the augmenting effect of surface imprinting of dopamine in polypyrrole over multiwalled carbon nanotubes (MWCNTs). To ensure the permselectivity of the probe towards dopamine molecules, a cation exchange polymer, nafion, is utilized as a membrane over imprinted sites to reduce the interference from anionic analytes like ascorbic acid and uric acid at physiological pH. The probe is characterized for a wide range of dopamine concentration from 0 to 10^{-5} M in artificial cerebrospinal fluid. Various probe parameters are varied to maximize the sensitivity of the sensor. The sensor possesses 18.9 pM as the limit of detection (LOD) which is lowest of those reported in the literature. The manifestation of sensing probe over an optical fiber along with the improved LOD makes the approach highly advantageous in terms of stability, repeatability, online remote monitoring, fast response, and miniaturization for its in vivo/in vitro applications in clinical sensing of dopamine.

1. Introduction

In a human body, neurons act as basic unit for communication and signal processing in brain through the exchange of some compounds known as neurotransmitters. Dopamine (DA) is one of such widely studied neurotransmitter being a critical component of central nervous system (CNS), cardiovascular and endocrine system (Demuru et al., 2018). Normal level of DA in brain is indicator of normal brain function, mood, emotion, movement and hormones. Excess of DA is responsible for the reward and pleasurable feelings whereas its deficiency leads to stress, depression, muscles and postural disorders. Thus, the release and uptake of DA in neural transmission is regarded as a biomarker for many neurocognitive disorders like Parkinson's disease, Schizophrenia, epilepsy, drug addiction, memory loss, attention deficit hyperactivity disorder and psychiatric problems. The normal concentration of DA in cerebrospinal fluid (CSF) is in the range 0.5–25 nM and in other physiological fluids like blood serum and urine is 0.1 μM (Jiang et al., 2017; Li et al., 2017). Owing to its important roles, continuous research is focused on its sensing and determination. Most of the conventional techniques used for its detection like HPLC and capillary electrophoresis suffer from the limitation of complicated instrumentation, time consumption and complex sample preparation (Moini et al., 2003). Electrochemical technique has also been reported in the literature for its determination owing to the advantages like fast response, high sensitivity and simple instrumentation. However, the similar oxidation potential of competing species like ascorbic acid (AA) and uric acid (UA) limits the selectivity of such technique (Liu et al., 2012). The optical techniques like SERS (Tang et al., 2015), fluorescence spectroscopy (Zhao et al., 2016), and absorbance spectroscopy (Feng et al., 2013) have also been reported for DA detection but are limited by low sensitivity, qualitative determination with lack of quantification, costly equipment, poor collection efficiency and poorly resolved peaks. Thus, the increased demand of new methodologies for the understanding of the role of DA in complex cerebral systems must simultaneously take into account the limitations of sensitivity, selectivity, antifouling, stability, reusability, cost effectiveness, fast and simple procedures for DA determination. The low concentration of DA in physiological environment and the presence of interferents like AA and UA require a highly sensitive methodology along with high selectivity probe for the accurate determination of DA concentration.

In recent years a combinational approach of surface plasmon resonance (SPR) and molecular imprinting technology has been used for

* Corresponding author.
E-mail address: bdgupta@physics.iitd.ac.in (B.D. Gupta).

https://doi.org/10.1016/j.bios.2019.03.023
Received 18 July 2018; Received in revised form 5 March 2019; Accepted 12 March 2019
Available online 13 March 2019
0956-5663/

the fabrication of a sensor to ensure the high sensitivity and selectivity of the analyte. The high sensitivity of SPR transduction mechanism relies on the highly sensitive response to the change in the dielectric constant of the layer adjacent to metal layer coated over the substrate such as prism and core of the optical fiber (Gupta et. al, 2009). The change in dielectric constant depends on the change in physicochemical properties of sensing layer due to its interaction with analyte. For the high sensitivity of the sensor the change in the dielectric constant of the sensing layer should be more for a given change in the concentration of the analyte. Therefore, the sensing layer in contact of metal layer is an important part of the SPR sensor. Another important property the sensing layer should have is that it should interact only with analyte to be detected so that the sensor can be specific to one particular analyte. Molecular imprinting is a breathtaking technology in the field of sensors to address specificity. It is applied on the sensing layer. In the conventional bulk imprinting, the artificial receptor sites are created in a cross-linked polymer matrix in the presence of template molecules through the covalent or non-covalent interaction. The template molecules are then leached out of the polymerized mixture, leaving behind complementary frozen locations specific for the adsorption of template molecules (Gupta et al., 2016). Apart from specificity, the molecular imprinting enhances the sensitivity to next level and provides smoothened adsorption and removal of template molecules. Surface imprinting based sensors require a complementing matrix material for the imprinting polymer along with the template molecule (Pathak et al., 2017).

In the present study, we report a SPR based fiber optic dopamine sensor fabricated using surface imprinted multiwalled carbon nanotubes (MWCNTs) matrix along with a cation exchange polymer, nafion, over the silver coated core of the fiber. Carbon nanotubes (CNTs) are chosen owing to their unique properties like boosting of charge transfer reactions at their surface, high mechanical stability, catalytic effects, very large surface to volume ratio and ease of surface modification (Kan et al., 2012). Polypyrrole (PPy) is one of the incessantly investigated conducting polymers for molecular imprinting due to its stability at neutral pH, ability to form a stable film around a variety of nanomaterials and easy chemical and electro-polymerization (Liu et al., 2011). Additionally, PPy offers a great choice of polymer for the imprinting of DA as the amine and hydroxyl groups in DA interact with oxygen containing groups on the oxidized PPy surface through hydrogen bonds forming highly stable and reproducible molecular imprinting polymer (MIP) films on the surface of CNTs (Tsai et al., 2012). The PPy/MWCNTs nanocomposite is used to improve the sensitivity and stability of the sensor as MWCNTs offers a conjugated π-bond structure with delocalized e^-s which provide easy interfacial interaction with PPy by reducing the system energy. To overcome the problem of false signaling from various analytes, a cation permeable nafion membrane is used over MIP sites. Various surfactants such as SDS (Chen et al., 2003), CTAB (Liu et al., 2012), polyglycine, tetraoctylammonium bromide, didodecyldimethylammonium bromide and nafion (Jeong and Jeon, 2008) to alert the interfacial properties and discriminate the differently charged species have been reported in the literature but we have chosen nafion after comparing its performance with other surfactants for ultra selective sensing of DA. Due to the cationic nature of DA ($pK_a = 8.9$) and anionic nature of AA ($pK_a = 4.04$) at physiological pH, nafion attracts DA and repel AA due to the presence of anionic sulfonic sites in its molecular chain. In short, a highly sensitive and extremely selective platform for the detection of DA is chosen by combining the high sensitivity of SPR systems, high selectivity of surface imprinted CNTs and minimal interference through additional nafion membrane over a fiber optic probe. The fiber optic platform adds to the advantages of the sensor due to its low cost, miniaturized probe, applications of in-vivo sensing combined with online monitoring.

2. Experimental

2.1. Reagents and Instruments

Plastic clad silica fiber with core diameter 600 μm and numerical aperture 0.4 was obtained from Fiberguide industries (USA). Silver wire (99% pure) for the coating of optical fiber was obtained from a local vendor in New Delhi. Pyrrole and multiwalled carbon nanotubes (MWCNTs) were obtained from Sigma Aldrich Pvt. Ltd. Hydrogen peroxide (H_2O_2) and iron (II) chloride ($FeCl_2$) used as oxidants for pyrrole polymerization were obtained from Merck India and Sigma Aldrich Pvt. Ltd. respectively. Dopamine hydrochloride (DAH), uric acid (AA), ascorbic acid, epinephrine and serotonin used as analytes and interferants for selectivity studies were also obtained from Sigma Aldrich Pvt. Ltd. Nafion perfluorinated resin used as cationic surfactant was obtained from Sigma whereas sodium dodecyl sulphate (SDS) and hexadecyltrimethylammonium bromide (CTAB) for surfactant studies were obtained from Merck India. Sodium dihydrogen phosphate dihydrate ($NaH_2PO_4{\cdot}2H_2O$) and disodium hydrogen phosphate ($Na_2HPO_4{\cdot}2H_2O$) for the preparation of buffer solution were also obtained from Merck India. Artificial cerebrospinal fluid (aCSF) was prepared using sodium chloride (NaCl), potassium chloride (KCl), magnesium sulphate ($MgSO_4$), sodium bicarbonate ($NaHCO_3$), calcium chloride ($CaCl_2$) procured from Merck India and the glucose, sucrose procured from CDH Pvt. Ltd. Reagents like ethanol, sulfuric and nitric acids were obtained from Merck India. The morphological characterization was performed on scanning electron microscope (SEM) (Zeiss EVO 50) and transmission electron microscope (TEM) (JEOL JEM-1400). UV–Vis measurements were carried out on Perkin Elmer Lambda 1050 spectrometer. In the experimental setup, tungsten halogen lamp (Model: Avalight-HAL) and the spectrometer (Model: Avaspec-3648) were purchased from AVANTES.

2.2. Preparation of nanocomposite

The preparation of nanocomposite involves three major steps. The first step involves the COOH functionalization of MWCNTs surface for their improved chemical interactions. For this, 10 mg of MWCNTs were dispersed in 3:1 ratio of H_2SO_4/HNO_3 mixture under ultra-sonication for 1 h. The mixture was refluxed at 90 °C for 12 h and sufficiently diluted and filtered using deionized (DI) water to obtain the carboxylic acid functionalized MWCNTs at neutral pH. The second step involves the formation of DA imprinted PPy shell around MWCNTs. A green-nano approach utilizing a mild oxidizing agent H_2O_2 in the presence of $FeCl_2$ was used for the facile synthesis of highly dispersed MWCNTs/PPy core shell structure via π-π interaction between MWCNTs and PPy (Liu et al., 2011). For the preparation of PPy/MWCNTs-MIP, 0.1 g of COOH-MWCNTs were dispersed in 100 ml DI water. 14 mM pyrrole was added to a pre-dispersed solution of COOH-MWCNTs and the assembly was stirred for 30 min. The polymerization was started with addition of 0.2 M H_2O_2 and 0.7 M $FeCl_2$ in the presence of various concentrations of DAH for forming the DA imprinted molecular sites. The polymerization lasted for 12 h with continuous stirring and the final products were collected by centrifugation and washing with DI water to remove unreacted reagents. To create the complementary sites for DA, the final products were eluted with ethanol: DI water (9:1) mixture for the removal of DA (Tsai et al., 2012). The complete removal was obtained after 4 steps of the elution and was confirmed by UV–Vis spectroscopy discussed in Section 3.2. Non-imprinted core-shell structure was obtained in the absence of DA following the same procedure for control experiments. The final step involves the covering of PPy/MWCNTs-MIP composite with cation exchange polymer, nafion. For this, 10 mg/ml of MIP composite was added to 1% nafion solution and mixed for 3 h (Hočevar et al., 2005). The complete schematic of nanocomposite preparation with chemical interactions involved is shown in Fig. 1(a).

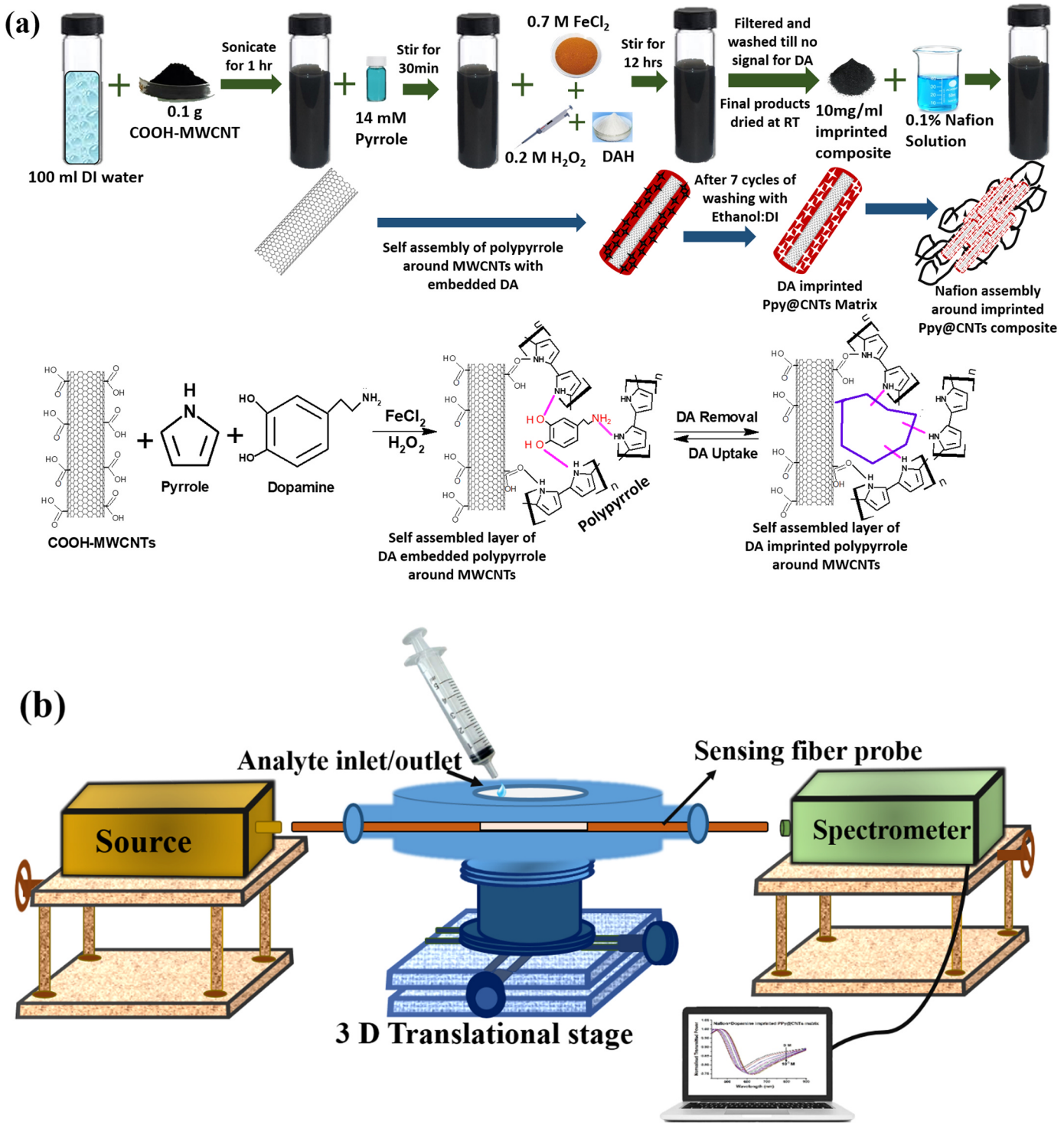

Fig. 1. (a) Schematic of steps and chemical interactions involved in nanocomposite preparation, and (b) experimental set-up.

2.3. Preparation of samples of artificial CSF with different dopamine concentrations

Cerebrospinal fluid (CSF) is an ultrafiltrate of plasma with extremely low cholesterol, protein, sugar and calcium, with no bilirubin and non-protein nitrogen but more of bicarbonate and chloride. The concentration of neurotransmitters in CSF is direct indicator of brain function and diseases. For medical diagnosis it is obtained from the spinal cord using lumbar puncture technique which involves certain health risks. However, imitation of CSF is extensively used for the research on DA determination (Ranc et al., 2014). For the present study, artificial CSF (aCSF) samples with different concentrations of DA ranging from 10^{-9} M to 10^{-5} M were prepared using phosphate buffer (Toledo et al., 2005). For the preparation of artificial CSF, 10 mM glucose, 4 mM sucrose, 2.5 mM $CaCl_2$, 26 mM $NaHCO_3$, 2 mM $MgSO_4$, 2.5 mM KCl and 124 mM NaCl were mixed. It may be noted that the constituents of CSF do not interfere with DA determination (Toledo et al., 2005).

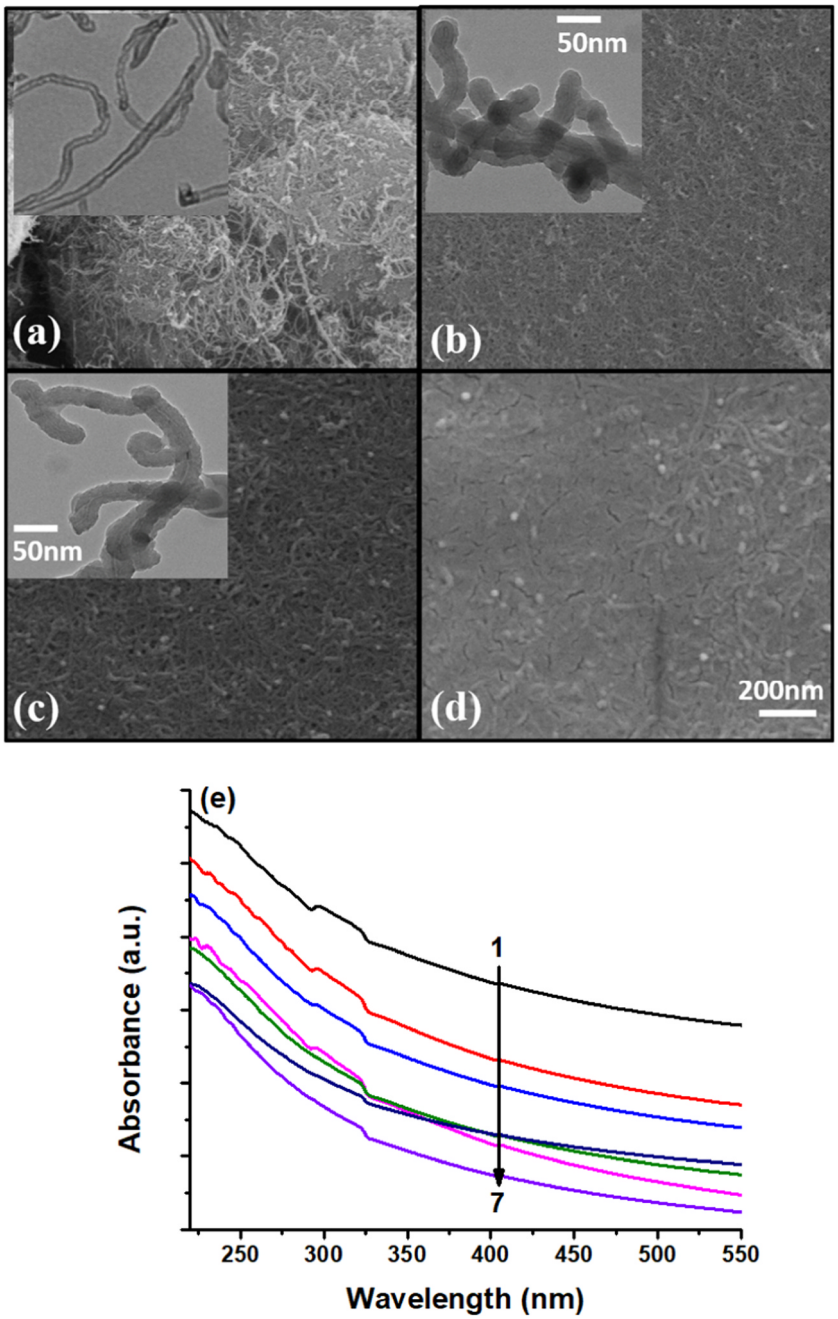

Fig. 2. SEM images of (a) MWCNTs, (b) dopamine embedded MWCNTs-PPy matrix, (c) dopamine imprinted MWCNTs-PPy matrix, and (d) Nafion/MWCNTs-PPy MIP nanocomposite. (e) UV–vis spectra of MWCNTs-PPy MIP nanocomposite during 7 elution steps with ethanol: DI water.

2.4. Preparation of fiber probe and experimental set-up

The fiber probe was prepared in two steps. The first step involves the coating of thin film of silver over unclad core of the fiber using thermal evaporation technique (Pathak et al., 2017). Silver, in place of gold, was used because of its low cost and high figure of merit (FOM). Figure of merit is the ratio of the sensitivity of the sensor to FWHM of the SPR curve and is better for the silver (Szunerits et al., 2008; Gupta and Verma et al., 2009). A 40 nm thin film of silver was coated over the 1 cm long unclad core of the fiber as it is the theoretically optimized thickness to get best SPR spectra. The thickness was controlled/measured with an inbuilt quartz crystal thickness monitor installed in the thermal evaporation coating unit. The second step involves the coating of PPy/MWCNT-MIP/nafion composite on the silver coated region of the probe using a dip coater at a fixed dipping/removal rate and for a particular dipping time. The removal speed and dipping time in the nanocomposite govern the thickness of the nanocomposite layer which affects the sensitivity of the probe. For the uniformity of the layer, the removal speed was kept low (1 mm/s) for all the probes. The uniformity was checked using the microscopic and SEM images. The thickness of the layer for 1 mm/sec of removal speed and 2 min of dipping time was found to be ~100 nm. The nanocomposite coated probe was dried at room temperature overnight and stored at 4 °C for experiments. The schematic of experimental set-up of the sensor is shown in Fig. 1(b). In the setup, the probe was fixed in a glass flow cell with facility of inlet/outlet of DA sample fixed on a 3d-translational stage for the light coupling. Both the ends of 12 cm long fiber probe were cleaved with tungsten cutter for better light coupling. Polychromatic light from the tungsten halogen lamp was launched at one end of the fiber to interact with the sensing region of the probe. The light exiting from the other

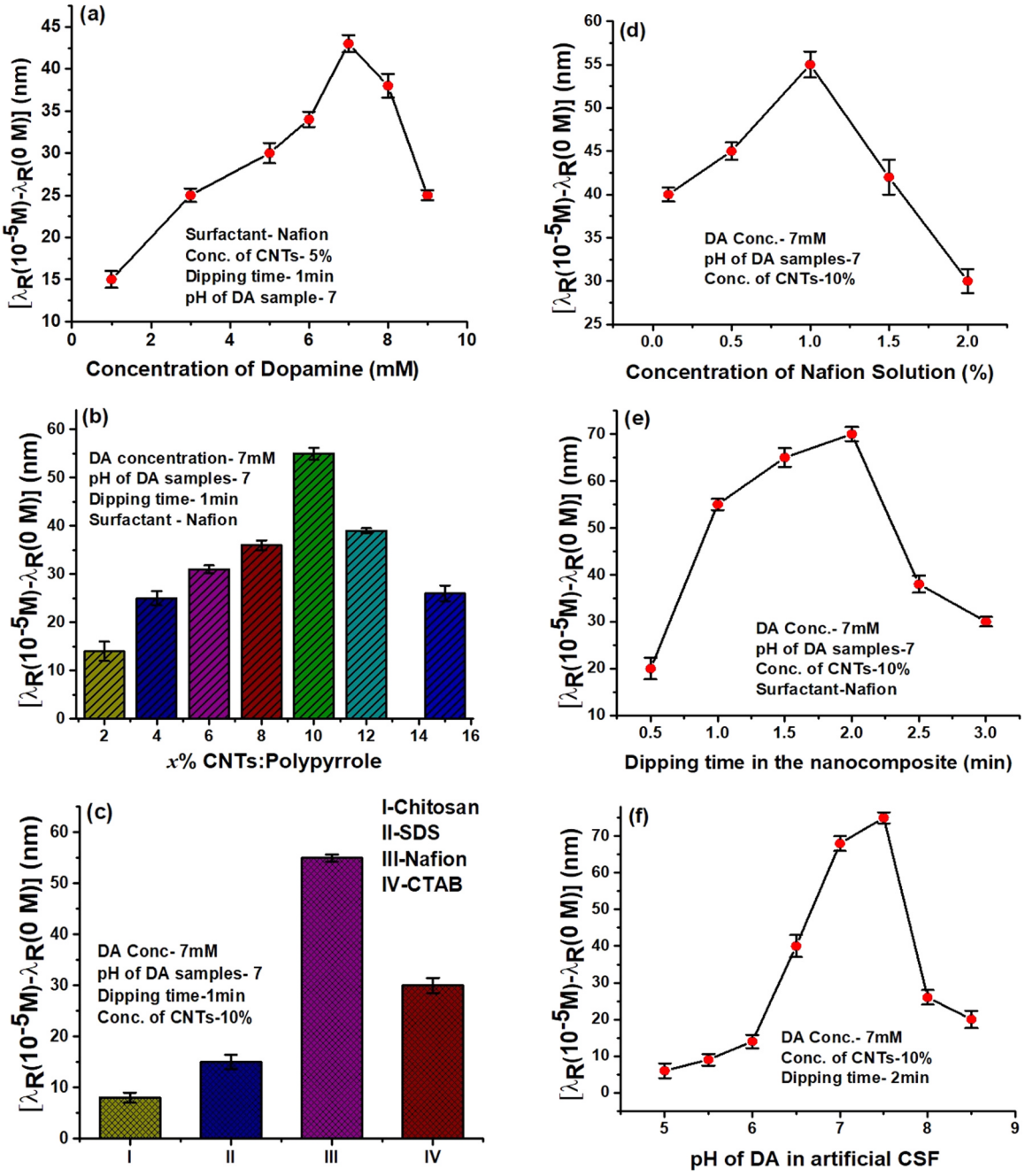

Fig. 3. Determination of (a) dopamine concentration in MIP nanocomposite, (b) weight percent of MWCNTs in nanocomposite, (c) surfactant for nanocomposite preparation, (d) nafion concentration, (e) dipping time of the probe in the nanocomposite, and (f) pH of the artificial CSF solution to achieve the maximum shift in resonance wavelength.

end of the fiber was collected by the spectrometer interfaced with the computer. The SPR spectra were recorded for the DA concentration from 0 M to 10^{-5} M. The probe was washed with DI water between two consecutive spectra.

3. Results and discussion

3.1. Sensing principle

SPR based sensors are designed on the fact that the resonance condition of SPR depends critically on the dielectric constant of the layer next to the metal layer (Sharma et al., 2007). In the case of chemical and biological sensors the change in the effective refractive index of the sensing layer occurs due to the chemical interaction/adsorption of the analyte with the sensing layer (Gupta and Verma, 2009). In the present study, the proposed probe is consisted of layers of silver as plasmonic material and Nafion/CNT-PPy-MIP as sensing layer where DA interacts with the artificially created DA sites on the sensing layer. As mentioned in the beginning, chemical polymerization method was used for the cross-linking of pyrrole monomer in the presence of DA over MWCNTs. The oxidized state of polypyrrole obtained in the present green synthesis procedure contains oxygen containing carbonyl and carboxyl groups in its backbone. The oxygen containing groups and –NH group of PPy bind with the electropositive amine group and hydroxyl group of DA respectively through hydrogen bonding. Thus, the present approach offers a robust polymerized medium through π-π

stacking of aromatic rings and hydrogen bonding between PPy and DA molecules (Teng et al., 2017; Tsai et al., 2012). The complementary sites are then created by elution of the composite with ethanol/DI water mixture. The interaction of DA molecules with these sites during sensing leads to the change in the effective refractive index of the MIP layer depending on the DA concentration (Gupta et al., 2016). Another important factor in sensors is the selectivity. Since DA is found in a very low concentration in physiological fluids compared to its interfering counterparts, AA and UA, the false signaling by these interfering analytes was avoided using a cation permeable membrane of nafion over the MIP coated MWCNTs. Nafion contains sulphate functional groups which attracts DA at physiological pH and repels anionic AA/UA due to electrostatic interaction (Chen et al., 2009).

3.2. Material characterization

The morphology of the nanocomposite was verified at each step by SEM images. From the image of MWCNTs shown in Fig. 2(a), a poor dispersibility of bundled untreated MWCNTs in DI water can be inferred. After functionalization and wrapping of MWCNT surface with PPy during nanocomposite preparation, their dispersibility significantly improves as evident from Fig. 2(b) showing the image of MWCNTs-PPy matrix embedded with DA molecules before MIP washing step. The enlarged TEM images, in inset, clearly show the formation of PPy film on CNT surfaces. Fig. 2(c) shows the final MWCNTs-PPy MIP composite after 7 steps of elution. No significant difference in the morphology of the composite is observed from Fig. 2(b) to (c). After wrapping of the MIP nanocomposite with cation exchange polymer, nafion, a thin permeable membrane formation at MIP surface can be seen in Fig. 2(d). Fig. 2(e) shows the UV–vis spectra of the surface imprinted nanocomposite at each washing step. It may be noted that the DA absorption peak around 290 nm is diminishing in each step. After 4 cycles of elution with ethanol/DI water solution a negligible peak of DA is observed which disappeared after 7 cycles of elution confirming complete removal of template from the imprinted nanocomposite (Ponzio and Ball, 2014).

3.3. Choice of probe fabrication parameters

The probe and nanocomposite fabrication involve many steps which need to be set to achieve the enhanced sensitivity of the sensor. To begin, the following parameters were chosen: concentration of CNT = 5%, dipping time = 1 min, pH of DA samples = 7, nafion as surfactant with 1% concentration and varying concentration of template. The motivation behind choosing these starting values was based on the literature survey. The procedure involves the recording of SPR spectra for DA samples of 0 and 10^{-5} M concentrations and from these the determination of shift in resonance wavelength for the change in dopamine concentration from 0 to 10^{-5} M.

3.3.1. Template concentration

The concentration of template molecule during the polymerization process in MIP decides the uniform distribution of imprinted sites in the polymer. If the concentration of template is less it may lead to decrease of sensitivity due to lesser number of interaction sites, whereas excess of template may result in distorted sites in the polymer (Usha and Gupta, 2018). To see the role of DA concentration during the in-situ polymerization of PPy at the surface of MWCNTs its concentration was varied from 1 mM to 9 mM. Fig. 3(a) shows the shift in resonance wavelength for the varying concentration of DA used in the preparation of MIP layer. A maximum shift of 43 nm in resonance wavelength is achieved for 7 mM concentration of DA in PPy-MWCNTs composite. The experiments were repeated 5–6 times to calculate the average value of the resonance wavelength shift and the standard deviation (error bar). Since the shift in resonance wavelength is directly related to the sensitivity of the sensor 7 mM concentration of DA was taken for the probe fabrication and obtaining the values of other parameters that give the maximum shift in resonance wavelength.

3.3.2. Percentage of MWCNTs in the nanocomposite

The present approach is based on imprinting of DA sites on the surface of MWCNTs through the chemical polymerization of PPy. A uniform wrapping of PPy around MWCNTs is required to achieve easily accessible imprinted sites. The lesser number of MWCNT results in insufficient number of surface imprinted sites as well as reduced charge transfer reactions which directly impacts the sensor sensitivity. Whereas an excess of MWCNTs may result in some non-wrapped CNTs providing an unstable dispersion. Hence, a suitable value of weight percentage of MWCNTs in the composite with respect to PPy was determined. For this, MWCNTs were varied from 2% to 15% and the measurements were taken similar to Fig. 3(a). As evident from Fig. 3(b), the shift in resonance wavelength increases from 2% to 10% and then decreases due to the reason mentioned above. A maximum shift of 55 nm was observed for 10% of MWCNTs in PPy.

3.3.3. Surfactant for the nanocomposite

For probe fabrication, four surfactants were exploited to cover surface imprinted composite to avoid the interference from AA and UA. Chitosan (Palanisamy et al., 2016), SDS (Chen et al., 2003), CTAB (Govindasamy et al., 2016) and nafion (Nagy et al., 1985) were tested as they are extensively reported for the DA sensing. Chitosan has positively charged groups on its surface, and hence repels most of the DA molecules and hence restricts their interaction with imprinted sites. The further experiments employ anionic surfactants SDS, nafion and CTAB. Fig. 3(c) shows the shift in resonance wavelength for all the four surfactants. Nafion gives the best performance with maximum shift of 55 nm in resonance wavelength. This is because nafion forms a cation permeable film over imprinted composite which reduces false signal from anionic interferants and is most compatible with our imprinted nanocomposite.

3.3.4. Concentration of nafion solution

To finalize the nafion concentration for the probe, 10 mg/ml of the imprinted composite was dissolved in varying volume percent solution of nafion. Maximum shift of 55 nm was obtained in the case of probe fabricated with 1% nafion solution in 0.05 M phosphate buffer as shown in Fig. 3(d). Large concentration of nafion forms a very thick layer around the composite which hampers the accessibility of the surface imprinted sites along with the formation of a very thick sensing layer around Ag coated core, which greatly affects the sensor sensitivity.

3.3.5. Dipping time in the nanocomposite

For the sensing of DA, layer of Nafion/MWCNTs-PPy-MIP nanocomposite was dip coated over the silver coated unclad core of the fiber. In dip coating method, the dipping time of the probe in the solution and its speed of removal from the solution decide the thickness of the layer. Since the performance of the SPR sensor relies on the evanescent field intensity at the interface of the sensing layer and analyte solution the thickness of the sensing layer becomes an important parameter (Shalabney and Abdulhalim, 2011). In other words, the electric field intensity at the interface greatly influences the sensitivity of the SPR sensor. This necessitates the determination of the dipping time of the probe in the nanocomposite solution which provides the best performance to the probe. For this, the dipping and removal speeds of the probe were kept as 5 mm/s to achieve a uniform and thin coating of the composite while the dipping time was varied from 30 s to 3 min. It is observed that for 2 min of dipping time, a maximum shift of 70 nm in resonance wavelength is obtained as evinced from Fig. 3(e).

3.3.6. pH of artificial CSF solution

The effect of pH of the artificial CSF solution on the sensing of DA was also studied. The pH of CSF was varied from 5 to 8.5. Fig. 3(f)

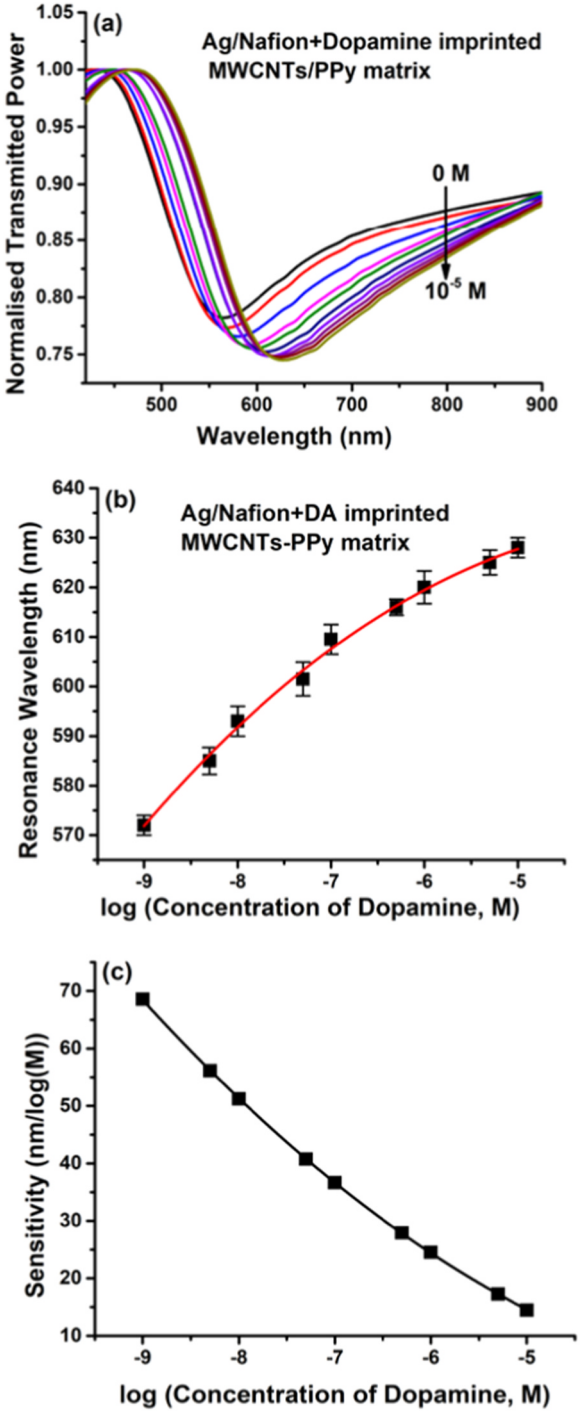

Fig. 4. (a) SPR spectra, (b) resonance wavelength, and (c) sensitivity for different concentrations of dopamine.

shows the maximum shift in resonance wavelength for 7.5 pH of the CSF which is close to the blood pH. The acidic pH not only makes the DA detection unstable due to its cationic nature but also results in fouling of the probe. Thus, a negligible sensor response is observed in acidic solution. On the other hand, basic pH condition not only results in self polymerization of DA to polydopamine but also results in the oxidation of catechol groups of DA to quinone form which affects the accurate concentration determination of DA (Zhou et al., 2014). Thus, neutral pH condition is found to be most suitable for DA detection and is also favorable physiologically.

3.4. Probe characterization

The probe fabricated with the parameters finalized above was characterized using the concentration of DA in the range from 0 to 10^{-5} M in aCSF and SPR spectrum was recorded for each concentration. Fig. 4(a) shows the SPR spectra for different concentrations of DA. It shows increase in resonance wavelength with the increase in DA concentration implying the increase in the effective refractive index of the sensing layer. The resonance wavelength extracted from each SPR spectrum is plotted in Fig. 4(b) as a function of DA concentration. The experiments were repeated 5–6 times and the average resonance wavelength was determined for each concentration. The standard deviation in resonance wavelength calculated for each concentration has been shown as error bar in the plot. It may be noted that the variation is nonlinear and saturates at higher concentration. The non-linear variation will be more clear if the resonance wavelength is plotted as a function of the concentration (and not logarithmic of concentration) of the dopamine. In Fig. 4(b), it appears to be linear due to logarithmic scale. The saturation is due to the fixed number of DA cavities on the sensing layer. As the concentration increases, the number of cavity available per DA molecule decreases and hence a decrease in the rate of change of resonance wavelength is observed. The sensitivity of the probe calculated taking the derivative of the calibration curve is shown in Fig. 4(c). The sensitivity decreases as the concentration of DA increases which clearly illustrates the maximum sensitivity at lowest concentration due to the reason described above. The maximum sensitivity of 68.58 nm/log (M) has been found for 10^{-9} M DA concentration in aCSF solution. The limit of detection (LOD) of the sensor was calculated as the thrice the ratio of standard deviation to sensitivity of the sensor near zero concentration (Chiavaioli et al., 2017; Tashkhourian and Dehbozorgi, 2016) and was found to be 18.9 pM. It is worth mentioning that this is only a calculated value obtained from the experimental results. The lowest concentration of DA utilized in the study was 1 nM.

3.5. Selectivity, stability, response time and control experiments

Selectivity is the key parameter to be addressed in the field of biosensors because of the presence of many interferants in the sample which can adversely affect the sensor performance. Hence, the probe was tested for interferants AA, UA, glucose, epinephrine (EP) and serotonin (SN) which co-exist with DA in our body. Three types of probes, MIP, NIP and MIP with nafion, were tested for the selectivity test. The shift in resonance wavelength was determined for the change in concentration from 0 to 10^{-5} M for all the interferants including DA. As evident from Fig. 5(a), AA and UA show a little shift in resonance wavelength with MIP and NIP based probes due to a possible chemical interaction with CNT-PPy matrix. The existence of their anionic forms at neutral pH makes them negligibly sensitive in the case of probe with nafion membrane due to electrostatic repulsion. EP and SN exist in cationic form at neutral pH and have similar structure as DA. But the specificity of MIP cavities for DA, makes the probe negligibly sensitive for EP and SN as evident from the quite similar shift in the case of MIP and NIP probes. Thus, the combined effect of specific molecular recognition sites prepared through MIP and the use of cation exchange polymer, nafion, in the preparation of sensing layer make the probe extensively selective for DA.

The repeatability of the probe was examined using DA concentrations of 0 M and 10^{-5} M. For this, 0 M solution was poured in the flow cell and SPR spectrum was recorded. The flow cell was then emptied and 10^{-5} M DA solution was poured to record the SPR spectrum after 1 min. The spectrum was recorded with a gap of 1 min for 3 times to check the stability of the probe. The resonance wavelengths so obtained are plotted in Fig. 5(b) for 3 cycles to check the repeatability of the probe.

The response time of the probe was also measured in a similar

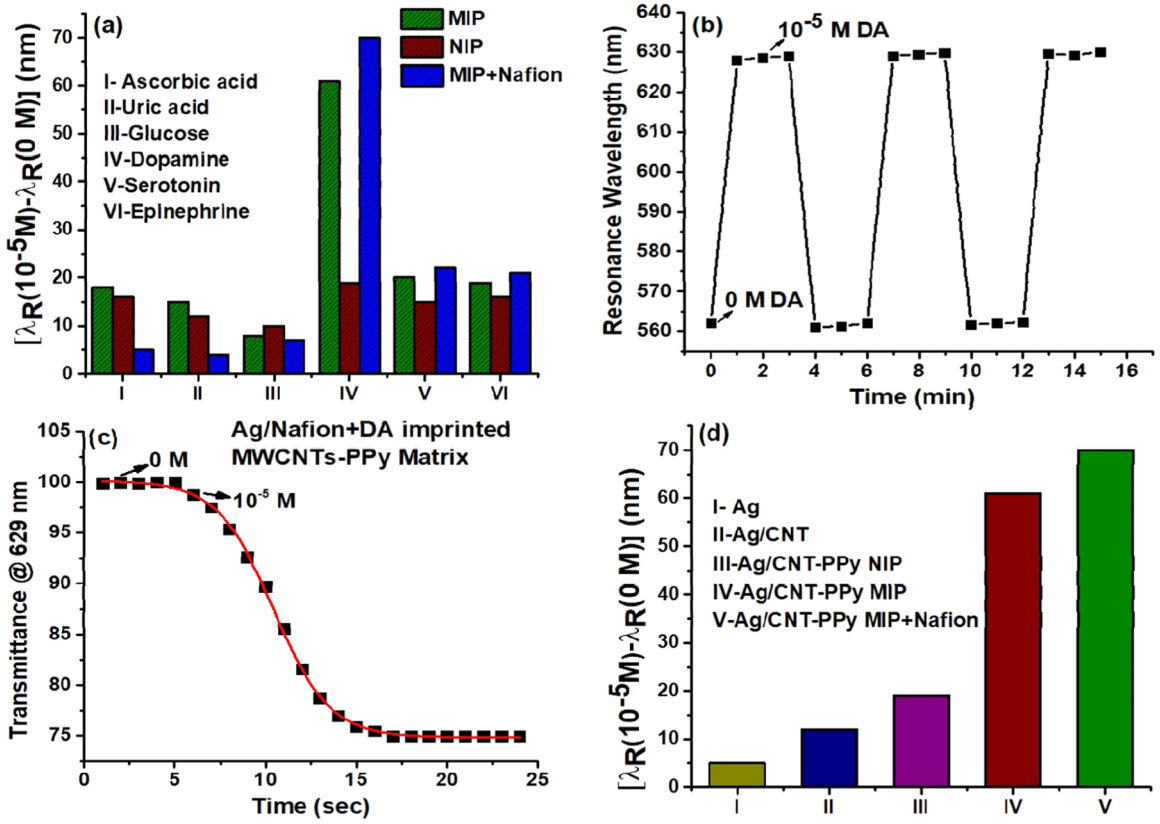

Fig. 5. Results of (a) selectivity, (b) repeatability, (c) response time, and (d) control experiments on the finalized probe.

manner. Response time depicts the time required for the stable response of the probe. For this study, the transmittance was recorded at a particular wavelength (629 nm) as a function of time as shown in Fig. 5(c) for 10^{-5} M DA concentration. The time response predicts the response time of the sensor close to 10 s. The transmittance recorded was fitted with Langmuir-Freundlich model which correctly depicts the binding in MIP technique (Umpleby et al., 2001).

Control experiments were performed to confirm the roles of each component of the sensing layer. For this, 5 different probes were fabricated and characterized for the sensing of DA as depicted in Fig. 5(d). The silver coated probe hardly shows any shift in resonance wavelength which confirms that the refractive index of all the DA solutions is same. A minor shift is observed for Ag/CNT and Ag/CNT-PPy (NIP) probes, which may be attributed to the minute adsorption of DA molecules on the surface of these probes. A significant shift of 61 nm is observed for MIP probe due to the interaction of DA molecules with the specifically created sites in the surface imprinted MWCNTs/PPY matrix. As seen from the figure, the addition of nafion layer provides a shift of 70 nm, which is quite similar to MIP probe. This manifests that nafion layer does not affect the sensitivity of the probe significantly but plays a crucial role in dopamine specific probe.

3.6. Comparison with other dopamine sensors

Several other techniques and materials have been used for the detection of dopamine in the literature. One such technique, electrochemical, has been used due to the electroactive nature of DA. The oxidation of AA and UA at potentials near to DA limits the selectivity of such sensor. Hence, several chemically and physically improvised electrodes have been examined for accurate and selective DA determination. One such approach based on electroimprinted (EIP) PPy nanowires uses voltammetry detection scheme (Teng et al., 2017). The EIP technology accounts for the acceptable selectivity and reproducibility of the scheme with LOD of 33 nM for the linear range 50 nM to 100 μM. Kan et al. (2012) have also reported a similar measurement methodology with an improvisation of surface electroimprinting of PPy on MWCNTs. The authors optimized various parameters like concentration of DA in MIP, scan rate for electropolymerisation, number of cycles for cyclic voltammetry (CV) for the best sensor performance. The surface imprinting improves the sensitivity through availability of easily accessible sites with dynamic range of 10^{-7} M to 10^{-4} M and 60 nM as LOD. Babaei and Taheri (2013) have utilized several voltammetry methods for nafion covered $Ni(OH)_2$/MWCNTs composite electrode over the range 0.05–25 μM of DA with LOD of 0.015 μM. $Ni(OH)_2$/MWCNT composite offers synergistic electrocatalysis effect to provide enhanced signals and low over potentials. The sensor provides repeatable stable response in 90 s. A chemically prepared CNT/PPy MIP composite over glassy carbon electrode (GCE) for DA detection has been used by Qian et al. (2014). The sensor possesses a wide dynamic range of 10^{-11} M to 10^{-6} M with 10 pM LOD. Template extraction for MIP has been performed through cyclic voltammetry (CV). The method provides a highly selective, sensitive and stable response without hindrance from common interferents like AA and UA with response time of 2 min due to specific imprinted sites for DA. However, these electrochemical methods suffer from the common limitation of electromagnetic (EM) noise and cannot be applied for in-vivo analysis. Most of the methods report a complicated electrochemical fabrication step as compared with our simple solution phase synthesis of MIP nanocomposite and its simpler dip coating on fiber probe. Moreover, the present study involves a wider dynamic range (10^{-9}–10^{-5} M) and lower or comparable LOD of 18.9 pM to these electrochemical approaches apart from the advantages like miniaturized fiber optic probe for in-vivo detection, no EM noise, easy measurement methodology and fast continuous online monitoring with typical response time of 10–15 s. Apart from these electrochemical techniques, Li et al. (2017) has reported a SERS based detection method

Table 1
Comparison of performance parameters of various dopamine sensors with present sensor.

Methodology	Materials	Dynamic Range	LOD	Ref.
Voltammetric	Electroimprinted PPy NWs	50 nM–100 μM	33 nM	Teng et al. (2017)
DPV and EIS	Electroimprinted PPy/MWCNTs	6.5×10^{-7}-10^{-4} M	60 nM	Kan et al. (2012)
DPV	Nafion/$Ni(OH)_2$ nanoparticles-CNT composite	0.05–25 μM	15 nM	Babaei and Taheri (2013)
Electrochemical	MIP based PPy/CNT composite	5×10^{-11}-5×10^{-6}M	10 pM	Qian et al. (2014)
SERS	AuNPs/CA-Fe(III) nanostructure on accupunture needles	0.1–100 nM	0.1 nM	Li et al. (2017)
Fluorimetric	Graphene Quantum Dots	0.01–50 μM	8.2 nM	Tashkhourian and Dehbozorgi (2016)
LSPR	Ag Nanoparticles	0–0.6 μM	60 nM	Lin et al. (2011)
SPR and Microcantilever	Oxaborole Polymer and Glycopolymer system	10^{-9}-10^{-4} M	10 pM	Jiang et al. (2017)
SPR	Ag film/Nafion/CNT-PPy MIP	10^{-9}-10^{-5} M	18.9 pM	This Work

for DA incorporating ferric citrate modified gold nanoparticles (AuNPs) on accupunture needles. SERS signals are reported to be fingerprints with high sensitivity for analyte. The sensor works for a narrow range of 0.1–100 nM of DA with response time of 1.5 min. In another fluorescence based approach, Tashkhourian and Dehbozorgi (2016) utilizes graphene quantum dots (GQDs) for the determination of DA over the range of 0.01–50 μM with LOD of 8.2 n M. The fluorescence based sensors are, however, limited by selectivity due to unavoidable changes in signal in the presence of other analytes. Lin et al. (2011) has reported a colorimetric and UV–Vis based approach utilizing DA stimulated aggregation of citrate capped silver nanoparticles (AgNPs). The approach is limited to the range 0–0.6 μM with 60 nM LOD. The main drawback of the proposed method is that it is based on Ag-catechol interaction in which the adsorbed DA molecules on AgNPs result in the reduction of their surface charge leading to their accumulation due to catechol moiety in DA. Thus, the approach is susceptible to false signals in the presence of catechol or catechol containing other molecules. Very recently, Jiang et al. (2017) has reported a conjugated polymer interface based on oxaborole polymer and glycopolymer for SPR and microcantilever (MCL) based DA sensors. The synthesis of such polymer interface is tedious compared to our simple surface MIP synthesis. Although the MCL based approach offers a better LOD of 50 pM, the SPR based approach has been found to be stable over a wider dynamic range with very fast response as compared to 5000 s response time of MCL system. Thus, the present study provides the benefits of highly sensitive SPR transduction mechanism in combination with ultraselective MIP and nafion based sensing layer. In addition to these, the fiber probe has advantages of perfectly miniaturized device as compared to prism based SPR method. The study has a faster response time of 10–15 s as compared to other reported methods in the literature with quite comparable LOD for clinical applications. The comparison of the performance of these methods has been summarized in Table 1 for better referral.

4. Conclusion

In conclusion, a contemporary approach is proposed and realized experimentally for the sensing of DA in aCSF utilizing combined effect of artificially created binding sites through MIP technique and a cation permeable nafion membrane along with highly sensitive technique of SPR. The probe exploits layers of silver for plasmonic excitation and MWCNTs wrapped with DA imprinted PPy covered in nafion membrane for sensing over the unclad core of the fiber. The sensor operates in the concentration range from 0 to 10^{-5} M of dopamine with highest sensitivity at lower concentration side making it appropriate for the diagnosis of Parkinson disease in real application scenario. To increase the sensitivity of the sensor, the values of various probe fabrication parameters are set. The finalized probe possesses a physiologically favorable LOD of 18.9 pM. Probe demonstrates stability, repeatability, selectivity and fast response to be applicable for real medical applications. Use of optical fiber substrate in probe design makes it feasible for online and remote monitoring along with the miniaturization required for in-vivo applications.

Declaration of interests

None.

Credit author statement

Both the authors have contributed equally.
Anisha Pathak and B.D. Gupta.

CRediT authorship contribution statement

Anisha Pathak: Conceptualization, Investigation, Methodology, Validation, Writing - original draft. **Banshi D. Gupta:** Supervision, Writing - review & editing, Validation.

References

Babaei, A., Taheri, A.R., 2013. Sens. Actuators B: Chem. 176, 543–551.
Chen, R.S., Huang, W.H., Tong, H., Wang, Z.L., Cheng, J.K., 2003. Anal. Chem. 75, 6341–6345.
Chen, P.Y., Vittal, R., Nien, P.C., Ho, K.C., 2009. Biosens. Bioelectron. 24, 3504–3509.
Chiavaioli, F., Gouveia, C.A.J., Jorge, P.A.S., Baldini, F., 2017. Biosensors 23, 1–29.
Demuru, S., Nela, L., Marchack, N., Holmes, S.J., Farmer, D.B., Tulevski, G.S., Lin, Q., Deligianni, H., 2018. ACS Sens. 3, 799–805.
Feng, J., Guo, H., Li, Y., Wang, Y., Chen, W., Wang, A., 2013. ACS Appl. Mater. Interfaces 5, 1226–1231.
Govindasamy, M., Chen, S.-M., Mani, V., Sathiyan, A., Merlin, J.P., Al-Hemaid, F.M.A., Ali, M.A., 2016. RSC Adv. 6, 100605–100613.
Gupta, B.D., Shrivastav, A.M., Usha, S.P., 2016. Sensors 16, 1381.
Gupta, B.D., Verma, R.K., 2009. J. Sens. 2009, 979761.
Hočevar, S.B., Wang, J., Deo, R.P., Musameh, M., Ogorevc, B., 2005. Electroanalysis 17, 417–422.
Jeong, H., Jeon, S., 2008. Sensors 8, 6924–6935.
Jiang, K., Wang, Y., Thakur, G., Kotsuchibashi, Y., Naicker, S., Narain, R., Thundat, T., 2017. ACS Appl. Mater. Interfaces 9, 15225–15231.
Kan, X., Zhou, H., Li, C., Zhu, A., Xing, Z., Zhao, Z., 2012. Electrochim. Acta 63, 69–75.
Li, P., Zhou, B., Cao, X., Tang, X., Yang, L., Hu, L., Liu, J., 2017. Chem. -A Eur. J. 23, 14278–14285.
Lin, Y., Chen, C., Wang, C., Pu, F., Ren, J., Qu, X., 2011. Chem. Commun. 47, 1181–1183.
Liu, S.Q., Sun, W.H., Hu, F.T., 2012. Sens. Actuators B: Chem. 173, 497–504.
Liu, Z., Liu, Y., Poyraz, S., Zhang, X., 2011. Chem. Commun. 47, 4421–4423.
Moini, M., Schultz, C.L., Mahmood, H., 2003. Anal. Chem. 75, 6282–6287.
Nagy, G., Gerhardt, G.A., Oke, A.F., Rice, M.E., Adams, R.N., Moore, R.B., Szentirmay, M.N., Martin, C.R., 1985. J. Electroanal. Chem. 189, 85–94.
Palanisamy, S., Thangavelu, K., Chen, S.M., Gnanaprakasam, P., Velusamy, V., Liu, X.H., 2016. Carbohydr. Polym. 151, 401–407.
Pathak, A., Parveen, S., Gupta, B.D., 2017. Nanotechnology 28, 355503.
Ponzio, F., Ball, V., 2014. Colloids Surf. A Physicochem. Eng. Asp. 443, 540–543.
Qian, T., Yu, C., Zhou, X., Ma, P., Wu, S., Xu, L., Shen, J., 2014. Biosens. Bioelectron. 58, 237–241.
Ranc, V., Markova, Z., Hajduch, M., Robert Prucek, R., Kvitek, L., Kaslik, J., Safarova, K., Zboril, R., 2014. Anal. Chem. 86, 2939–2946.
Shalabney, A., Abdulhalim, I., 2011. Laser Photonics Rev. 5, 571–606.
Sharma, A.K., Jha, R., Gupta, B.D., 2007. IEEE Sens. J. 7, 1118–1129.

Szunerits, S., Castel, X., Boukherroub, R., 2008. J. Phys. Chem. C 112, 15813–15817.
Tang, L., Li, S., Han, F., Liu, L., Xu, L., Ma, W., Kuang, H., Li, A., Wang, L., Xu, C., 2015. Biosens. Bioelectron. 71, 7–12.
Tashkhourian, J., Dehbozorgi, A., 2016. Spec. Lett. 49, 319–325.
Teng, Y., Liu, F., Kan, X., 2017. Microchim. Acta 184, 2515–2522.
Toledo, R.A., Santos, M.C., Cavalheiro, E.T.G., Mazo, L.H., 2005. Anal. Bioanal. Chem. 381, 1161–1166.
Tsai, T.C., Han, H.Z., Cheng, C.C., Chen, L.C., Chang, H.C., Chen, J.J.J., 2012. Sens. Actuators, B: Chem. 171–172, 93–101.
Umpleby, R.J., Baxter, S.C., Chen, Y., Shah, R.N., Shimizu, K.D., 2001. Anal. Chem. 73, 4584–4591.
Usha, S.P., Gupta, B.D., 2018. Biosens. Bioelectron. 101, 135–145.
Zhao, J., Zhao, L., Lan, C., Zhao, S., 2016. Sens. Actuators B: Chem. 223, 246–251.
Zhou, X., Ma, P., Wang, A., Yu, C., Qian, T., Wu, S., Shen, J., 2014. Biosens. Bioelectron. 64, 404–410.